Deterministic hopping in a Josephson circuit described by a one-dimensional mapping

Robert F. Miracky,* Michel H. Devoret,† and John Clarke
Department of Physics, University of California, Berkeley, California 94720
and Materials and Molecular Research Division, Lawrence Berkeley Laboratory, Berkeley, California 94720
(Received 9 November 1984)

Analog simulations of the hopping noise of a current-biased Josephson tunnel junction shunted with an inductor in series with a resistor reveal a $1/\omega$ spectral density over two decades of frequency ω for a narrow range of bias currents. The amplitude of the low-frequency part of the spectrum decreases when white noise, representing Nyquist noise in the resistor at a few degrees Kelvin, is added to the simulation. We explain the shape of the power spectrum and its dependence on bias current and added white noise in terms of a deterministic process, involving a one-dimensional mapping, that is analogous to that found in Pomeau-Manneville intermittency. Moreover, we are able to establish a detailed relationship between the origin of the mapping and the differential equation describing the dynamics of the system.

I. INTRODUCTION

A major advance was made in the field of nonlinear dynamics when it was shown that a nonlinear dissipative system with only a few degrees of freedom could exhibit noise produced in a deterministic way[1] (chaos). Thus, the long-term unpredictability of certain systems can have its origin in the particular structure of the nonlinear differential equations governing these systems and not in the fact that they interact with a very large number of degrees of freedom. At the same time, a deeper understanding of some of the mechanisms producing chaos was gained when it was realized how the iteration of a simple one-dimensional mapping of an interval of real numbers into itself could produce chaotic behavior for a particular range of parameters.[2]

The question then arose as to whether it is possible, in some cases, to reduce the set of differential equations governing a physical system to the iteration of a simple mapping, and thus to identify the chaos-producing mechanism in this system. This question has been answered in a particular type of chaotic phenomenon called the Pomeau-Manneville intermittency.[3] In general, intermittency, which is the occurrence of noise in bursts, can have many different origins, but in the particular class studied by Pomeau and Manneville it occurs when a physical system in a limit cycle becomes unstable and undergoes a Hopf bifurcation.[4] For the intermittency to occur, the limit cycle must lose its stability to a chaotic attractor. At the onset of instability, the system is in the limit cycle for periods of time which are interrupted in a seemingly random fashion by bursts of noise. Pomeau-Manneville intermittency can be understood in terms of the Poincaré map of the equations of the system in the neighborhood of the limit cycle. This Poincaré map reduces to a mapping of the complex plane onto itself with the generic form $z \rightarrow z(1+\epsilon)e^{i\lambda} +$ (higher-order terms), where $\epsilon \rightarrow 0^+$ corresponds to the onset of intermittency. Providing that the Poincaré map reinjects points at random in the vicinity of $z=0$, the long-time chaotic behavior is entirely determined by the real numbers ϵ and λ. This mechanism has been shown to occur in several physical systems.[5,6]

It would be interesting to know if this complete understanding of noise in one particular case can be achieved in other cases. A commonly encountered type of noisy behavior is hopping, the apparently random transition of a dynamical variable among several distinct states. (Intermittency can be thought of as a limiting case of hopping between two states, a noise-free state and a noise-producing state.) Hopping is a general phenomenon which is found in a variety of nonlinear physical systems such as optical devices,[7] semiconductor devices,[8] electrical circuits,[9,10] and Josephson junctions.[11]

In this paper we will focus on the hopping phenomenon found in Josephson junctions. Josephson junctions have the advantage of being a "minimal" nonlinear chaotic system: They can be represented by a set of first-order differential equations with only three variables, the minimal number required for the observation of chaos.[12] They also lend themselves easily to real experiments and analog simulations, as well as to numerical simulations.

This article demonstrates that a particular type of hopping exhibited by a Josephson junction shunted by a resistance having substantial self-inductance can be explained deterministically via a one-dimensional mapping by the equations of motion of the junction. The paper is organized as follows. Section II reviews the different types of chaotic behavior that have been found in Josephson junctions, with emphasis on a particular type of hopping between two modes that is suppressed by the addition of noise and that exhibits an excess low-frequency noise (deterministic hopping). Section III investigates the relationship between the frequency dependence of the spectrum and the statistical properties of the time intervals between hopping events which may provide some indication of the mechanism producing hopping. As an example of such a mechanism, we describe a mathematical model which is completely deterministic and produces a $\omega^{-\nu}$ spectrum (ω is the frequency). In Sec. IV we analyze the differential equations of the system with a computer

simulation using the method of Poincaré sections.[13] The Poincaré section of the flow is a strange attractor which can be divided into two regions corresponding to the two modes between which the system hops back and forth. Section V shows how the flow in one region can be used to construct a one-dimensional mapping that demonstrates one of the transitions between the two modes. The relationship between this mapping and the mathematical model developed in Sec. II is discussed. Section VI contains a concluding summary.

II. THE HOPPING PHENOMENON IN A JOSEPHSON JUNCTION

A Josephson tunnel junction consists of two superconductors separated by a thin insulating barrier through which pairs of electrons (Cooper pairs) can tunnel coherently.[14] The supercurrent I_S through the junction is determined by the relation

$$I_S = I_0 \sin\delta \ , \tag{2.1}$$

where I_0, the critical current, is the maximum supercurrent that the junction can sustain without developing a voltage, and δ is the phase difference between the complex order parameters in the two superconductors. For applied currents greater than I_0, part of the current must flow through a resistive element (intrinsic to the junction or added externally) so that a voltage V is developed across the junction. In this state, Eq. (2.1) is still valid, but $\delta(t)$ evolves with time according to the relation

$$V = (\Phi_0/2\pi)\dot{\delta} \ , \tag{2.2}$$

where $\Phi_0 \equiv h/2e$ is the flux quantum and the dot represents differentiation with respect to time. The two other intrinsic parameters of the junction are its self-capacitance C, formed by the overlap of the two superconductors, and its nonlinear quasiparticle conductance $\sigma_{qp}(V) = I_{qp}/V$, where I_{qp} is the quasiparticle current.

Chaos in Josephson junctions has been studied in several circuits. In the most widely studied, a Josephson junction shunted by its self-capacitance and a resistor is driven with an alternating current.[15–17] This system is governed by the same second-order nonautonomous equation as the driven, damped pendulum, namely

$$\ddot{\delta} + \gamma\dot{\delta} + \Omega_0^2 \sin\delta = a\cos(\Omega t) \ , \tag{2.3}$$

where $\Omega/2\pi$ is the frequency of the driving current. In particular, hopping between metastable states has been observed in simulations,[11,16–19] and has recently been observed experimentally.[20] In one of these studies, Ben-Jacob *et al.*[11] analyzed Eq. (2.3) for parameter values for which there is hopping between two unstable phase-locked states. Their analytical calculation of a simplified model of Eq. (2.3) produces power spectra that decay as $1/\omega^2$ or $1/\omega^4$ (depending on parameter values) at relatively high frequencies. Their numerical computations are in good agreement with their analysis. In a similar vein, Geisel *et al.*[18] have also analyzed Eq. (2.3), together with a related one-dimensional mapping, and found a $1/\omega^2$ dependence above some characteristic frequency. Very recently, Gwinn and Westervelt[19] presented numerical simulations of Eq. (2.3) showing $1/\omega$ noise over a limited range, but found that this noise is easily destroyed by a small amount of computational noise.

We have studied in detail an alternative circuit, shown in Fig. 1, both experimentally and in simulations.[21,22] Here, the junction is shunted externally with a resistance R in series with an inductance L and is biased with a steady current. The application of Kirchhoff's laws to the circuit shown in Fig. 1 yields the equations

$$I = I_0 \sin\delta + (\Phi_0/2\pi)C\ddot{\delta} + I_S + I_{qp} \tag{2.4}$$

and

$$(\Phi_0/2\pi)\dot{\delta} = RI_S + L\dot{I}_S + V_N \ , \tag{2.5}$$

where $V_N(t)$ is the thermal voltage noise generated by the resistance R; since $R \ll 1/\sigma_{qp}$ for situations of practical interest, we neglect the thermal noise voltage associated with σ_{qp}. To simplify the situation, we assume that σ_{qp} is linear over the voltage range of interest with the dimensionless value $\sigma = R\sigma_{qp}$. It is more convenient to write Eqs. (2.4) and (2.5) in dimensionless form. If we introduce a dimensionless time $\tau = (2\pi I_0 R/\Phi_0)t$, Eqs. (2.4) and (2.5) become

$$i = \sin\delta + \beta_C\ddot{\delta} + i_S + \sigma\dot{\delta} \tag{2.6}$$

and

$$\dot{\delta} = i_S + \beta_L\dot{i}_S + v_N \ , \tag{2.7}$$

where $i = I/I_0$, $i_S = I_S/I_0$, $v_N = V_N/I_0R$, $\beta_C = 2\pi I_0 R^2 C/\Phi_0$, and $\beta_L = 2\pi L I_0/\Phi_0$. The dots now denote differentiation with respect to τ. The magnitude of the voltage noise is characterized by $\Gamma = 2\pi k_B T/I_0\Phi_0$, the ratio of thermal noise to the junction coupling energy.

Although there has been some analytical work on the dynamics of this system—Wiesenfeld *et al.*[23] have calculated to good accuracy the threshold for the first period-doubling bifurcation as the bias current i is reduced from some large value—most of the insight into the complicated dynamics of the system has been achieved with both analog and digital simulations.[21,22] Measurements of the low-frequency noise developed by this system revealed excessive amounts of noise (with a power 10^5 or more times larger than the Nyquist noise at 4 K, and 10^2 to 10^3 times larger than "chaotic noise") over small intervals of bias current for which there is hopping between limit cycles or between a limit cycle and a chaotic regime. Analog simulations showed that this hopping produced a low-frequency noise power spectrum that varied approximate-

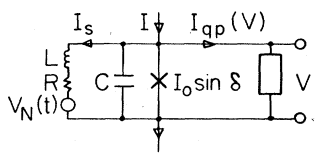

FIG. 1. Schematic representation of Josephson tunnel junction with critical current I_0 and self-capacitance C shunted with an external resistance R which has self-inductance L; I_{qp} is the quasiparticle tunneling current and V_N is the Nyquist voltage noise associated with the resistance.

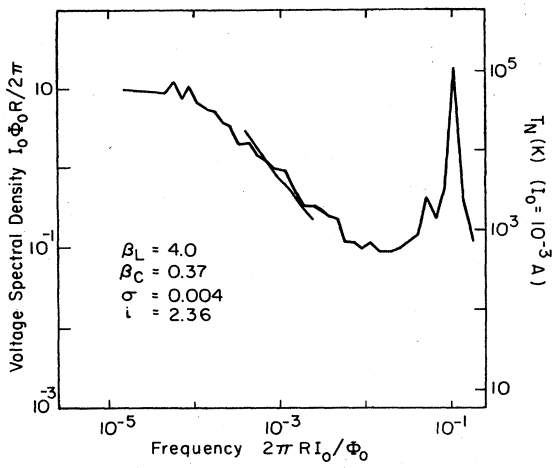

FIG. 2. Voltage power spectrum for an electronic analog of the circuit shown in Fig. 1, with parameters chosen to maximize the $1/\omega$ region: $\beta_L=4.0$, $\beta_C=0.37$, $\sigma=0.004$, $i=2.36$, and $\Gamma=3\times10^{-7}$. (The spectrum was computed over two overlapping frequency intervals.)

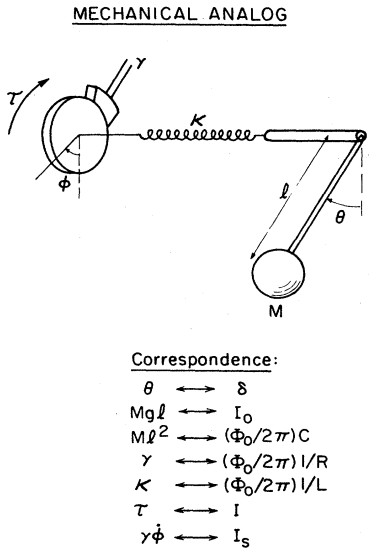

FIG. 3. Mechanical analog of a Josephson junction shunted with a resistance in series with an inductance (circuit of Fig. 1); τ is the applied torque, γ is the friction coefficient, and κ is the torsional constant.

ly as $1/\omega$ over typically two decades, and that the hopping was induced by the Nyquist noise in the shunt resistance. Thus, when the Nyquist noise was reduced to a very low level in the simulation, the hopping process ceased, and the low-frequency $1/\omega$ noise vanished. However, in the course of this survey of the various chaotic regimes, a relatively rare situation was observed in which a low-frequency $1/\omega$ power spectrum (also over as much as two decades) was produced by hopping that occurred in the *absence* of thermal noise. This process, which we refer to as *deterministic hopping* for reasons that will appear later, occurred only at very precisely chosen values of the bias current, and was *destroyed* by the application of a modest level of Nyquist model.

Figure 2 shows a voltage power spectrum obtained from an electronic analog[24] of the circuit shown in Fig. 1 for one set of parameter values ($\beta_L=4.0$, $\beta_C=0.37$, $i=2.36$, $\sigma=0.004$) where this excess low-frequency noise was observed. There was no added voltage noise, and the intrinsic noise of the analog was estimated to be less than 7 mK. The spectrum scales approximately as $1/\omega$ between the dimensionless frequencies 10^{-4} and 10^{-2}, and is seen to flatten out below 10^{-4}. The large peak near 10^{-1} and the one slightly lower in frequency correspond to residual subharmonic modes. Their linewidths are in fact narrower than is apparent: The broadening is an artifact of an averaging of adjacent Fourier harmonics.

By monitoring the time sequence of the voltage, we conclude that this low-frequency noise originates in a two-model hopping process, rather than in some other process. The steady-state waveform spends random-time intervals in one of two distinct nearly-periodic modes that differ in one important aspect. While in one mode δ increases monotonically with time (i.e., $\dot{\delta}>0$), in the other δ becomes periodically negative. Although the latter behavior is impossible for $\beta_L=0$, it occurs commonly for $\beta_L\geq1$ and represents a "relaxation oscillation."[25] In this mode, the junction oscillates for a while at the Josephson frequency (determined by the voltage across the junction), and then relaxes to a state with zero-average voltage in which the junction undergoes damped oscillations at the plasma frequency,[14] $\omega_p=(2\pi I_0\cos\delta/\Phi_0C)^{1/2}$. The junction subsequently returns to the nonzero voltage regime, and the cycle repeats.

An intuitive picture of the two modes is provided by the pendulum analog of the Josephson junction shown in Fig. 3. The correspondence between the two sets of parameters is listed in the figure. The pendulum pivots about an axle attached to a spring with torsional constant κ, the other end of which is driven with a constant torque τ. Thus, one can store energy in both the pendulum (which corresponds to the junction) and the spring (which corresponds to the inductance). Frictional loss γ is provided by a brake (which corresponds to the resistance). When the applied torque is sufficiently large compared with the critical torque Mgl, θ will advance monotonically ($\dot{\delta}>0$ for the junction). This situation is similar to an automobile clutch when it is "engaged." On the other hand, for lower values of torque, one can envision the pendulum occasionally falling backwards ($\dot{\delta}<0$ for the junction), much like a "slipping" clutch, and undergoing several small oscillations at angular frequency $(g/l)^{1/2}$ before again executing a complete revolution. Bearing in mind this analog, we label the mode for which $\dot{\delta}$ is always positive the "engaged mode" and that in which relaxation oscillations occur the "slipping mode."

An important aspect of the hopping process is that, unlike the situation described in Ref. 21, it occurs in the absence of added white (Nyquist) noise. Although the residual white noise in the electronic analog, estimated to be $\Gamma=3\times10^{-7}$ (equivalent to a Nyquist noise at about 7 mK for $I_0=1$ mA), cannot be entirely ruled out as a source of

the hopping, we found that the low-frequency power spectrum was not significantly affected until we added a noise equivalent to several hundred milliKelvin. Furthermore, we found that the power spectrum was much more sensitive to the value of the bias current than is the case for the noise-induced hopping. Both of these results suggest that the switching arises deterministically from the governing equations, as will become clearer in the next section. We note that for the deterministic hopping, the $1/\omega$ noise was relatively insensitive to the values of β_C and β_L, either of which could be varied over a range of perhaps 10% to 20% before the hopping ceased.

To understand the particular frequency dependence of the spectrum it is important to note that the two modes are characterized by two different *average* voltages. The long-time behavior of the signal is thus dominated by the hopping between these two voltages and it is the statistical properties of the time interval between two hopping events that determine the low-frequency spectrum. The exact relationship between these statistical properties and the spectrum is investigated in the next section, together with a deterministic model that has statistical properties leading to a $1/\omega$ power spectrum.

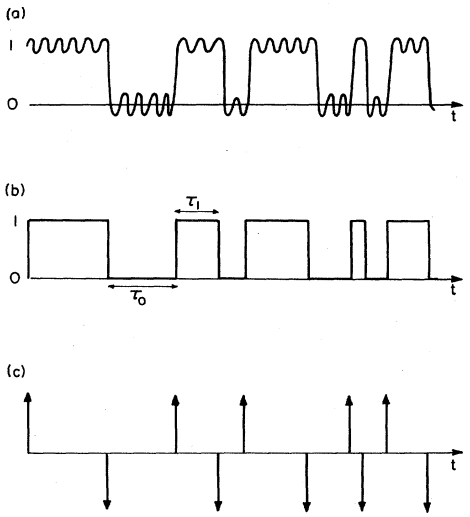

FIG. 4. (a) Time sequence of a signal showing switching between two distinct oscillatory modes; (b) time sequence obtained from (a) by retaining only the zero-frequency component of each mode; (c) derivative of the time sequence in (b)—the arrows represent delta functions.

III. SPECTRAL DENSITY OF HOPPING NOISE: DETERMINISTIC MODEL PRODUCING HOPPING NOISE WITH A $\omega^{-\nu}$ SPECTRAL DENSITY

In this section we calculate the spectral density of a simple two-state hopping process as a function of the probability distribution of the time intervals between hopping events. We obtain sufficient conditions for the observation of a $\omega^{-\nu}$ power spectrum and describe a mathematical deterministic model based on the iteration of a one-dimensional mapping that satisfies these criteria.

A. Simple model for switching noise

We consider a physical process in which a variable hops between two states of the system as indicated in Fig. 4(a). Each state represents some dynamical process, for example, a fixed point, a limit cycle, or a chaotic regime. We assume that the characteristic frequencies of these dynamical processes are much higher than typical hopping frequencies between the two states, so that each state may be represented by a time-averaged value as shown in Fig. 4(b). Thus, we need consider only a signal $x(t)$ that takes the values 0 and 1 during successive random intervals τ_0 and τ_1. We assume that all the intervals are statistically independent of one another. The random process is thus described entirely by the probability distributions

$$\pi_0(t)=\text{Prob}\ (\tau_0>t)\ ,$$
$$\pi_1(t)=\text{Prob}\ (\tau_1>t)\ . \tag{3.1}$$

The interesting property of our model, as we shall see, is that the spectral density $S_x(\omega)$ of the process $x(t)$ can be calculated in closed form in terms of $\pi_0(t)$ and $\pi_1(t)$. When $\pi_0=\pi_1$, the process is completely described by its power spectrum (as is the case, for example, for Gaussian noise).

B. Calculation of spectral density

Our procedure is to compute the correlation function $G(t)$ of the time derivative $y(t)=dx(t)/dt$, and to Fourier transform this correlation function to obtain the spectral density $S_y(\omega)$. We then use the result

$$S_x(\omega)=S_y(\omega)/\omega^2\ . \tag{3.2}$$

We chose this method because the calculation of the correlation function of $y(t)$, which consists of delta functions of alternating sign [Fig. 4(c)], is particularly simple.

It can easily be shown that

$$\begin{aligned} G(t)&\equiv\langle y(0)y(t)\rangle \\ &=\langle\,|y(0)|\,\rangle\{\delta(t)+\tfrac{1}{2}[\langle y(t)\rangle_+-\langle y(t)\rangle_-]\} \\ &=[2/(\langle\tau_0\rangle+\langle\tau_1\rangle)]g(t)\ , \end{aligned} \tag{3.3}$$

where, assuming $y(t)$ is stationary, $\langle y(t)\rangle_\pm$ is the ensemble average value of $y(t)$ at time t when there is a spike of sign $\pm$ at $t=0$. The quantity $\langle\,|y(0)|\,\rangle$ is simply the average rate of spikes at $t=0$. If necessary, stationarity can be imposed by introducing a cutoff at long times in $\pi_0(t)$ and $\pi_1(t)$.

We define the probability densities $p_0(t-t')$ and $p_1(t-t')$ of finding a positive and negative delta function, respectively, at time t when there is a negative and positive delta function at time t':

$$p_0(t)=\frac{d}{dt}[1-\pi_0(t)]\ ,$$

and

$$p_1(t)=\frac{d}{dt}[1-\pi_1(t)]\ . \tag{3.4}$$

One then finds

$$\langle y(t)\rangle_+ = -p_1(t) + \int_0^t dt' p_0(t-t')p_1(t') - \int_0^t dt' p_1(t-t') \times \int_0^{t'} dt'' p_0(t'-t'')p_1(t'') + \cdots , \quad (3.5)$$

together with an analogous expression for $\langle y(t)\rangle_-$ by interchanging 0 and 1 and + and − in Eq. (3.5). The nth term in this infinite series corresponds to the situation in which there are n delta functions between 0 and t.

We can resum these series expansions using Laplace transforms

$$\mathcal{L}\{f(t)\} = \tilde{f}(z) = \int_0^\infty e^{-zt} f(t)dt , \quad (3.6)$$

and making use of the property

$$\mathcal{L}\left\{ \int_0^t dt' f(t-t') \int_0^{t'} dt'' g(t'-t'') \right\} = \tilde{f}(z)\tilde{g}(z) . \quad (3.7)$$

We obtain

$$\mathcal{L}\{\langle y(t)\rangle_+\} = -\tilde{p}_1(z) + \tilde{p}_0(z)\tilde{p}_1(z) - \tilde{p}_1(z)\tilde{p}_0(z)\tilde{p}_1(z) + \cdots = \frac{-\tilde{p}_1 + \tilde{p}_0\tilde{p}_1}{1-\tilde{p}_0\tilde{p}_1} , \quad (3.8)$$

and a similar expression for $\langle y(t)\rangle_-$. Subtracting the two expressions and rewriting the result in terms of $\tilde{\pi}_0(z)$ and $\tilde{\pi}_1(z)$, we obtain

$$\tilde{g}(z) = \tfrac{1}{2}\{z^{-1}[\tilde{\pi}_0^{-1}(z) + \tilde{\pi}_1^{-1}(z)] - 1\}^{-1} . \quad (3.9)$$

We can easily compute the Fourier transform, $\tilde{g}(\omega)$, of $g(t)$ from the result

$$\tilde{g}(\omega) = \int_{-\infty}^{\infty} e^{-i\omega t} g(t)dt = \lim_{z \to i\omega} [\tilde{g}(z) + \tilde{g}(\bar{z})] , \quad (3.10)$$

where $\bar{z}$ is the complex conjugate of z. Finally, we obtain the required spectral density of $x(t)$

$$S_x(\omega) = \frac{2}{\langle \tau_0 \rangle + \langle \tau_1 \rangle} \frac{\tilde{g}(\omega)}{\omega^2} . \quad (3.11)$$

C. Self-similar power spectra

We are now in a position to determine the conditions that must be satisfied by $\pi_0(t)$ and $\pi_1(t)$ so that the power spectrum $S_x(\omega)$ diverges in the limit $\omega \to 0$ as $A\omega^{-\nu}$, where A and ν are positive constants. We restrict ourselves to distributions that have a well-defined power-law behavior as $t \to \infty$. To leading order, we take

$$\pi_0(t) \sim a_0 t^{-\beta_0} \text{ as } t \to \infty, \ \beta_0 > 0 ,$$
$$\pi_1(t) \sim a_1 t^{-\beta_1} \text{ as } t \to \infty, \ \beta_1 > 0 . \quad (3.12)$$

Exponentially decreasing distributions can be treated by letting $\beta \to \infty$. Using Eq. (3.9) and tables of Laplace transforms,[26] we obtain the values of ν as a function of β_0 and β_1 listed in Table I. A plot of ν versus β_0 and β_1 is given in Fig. 5.

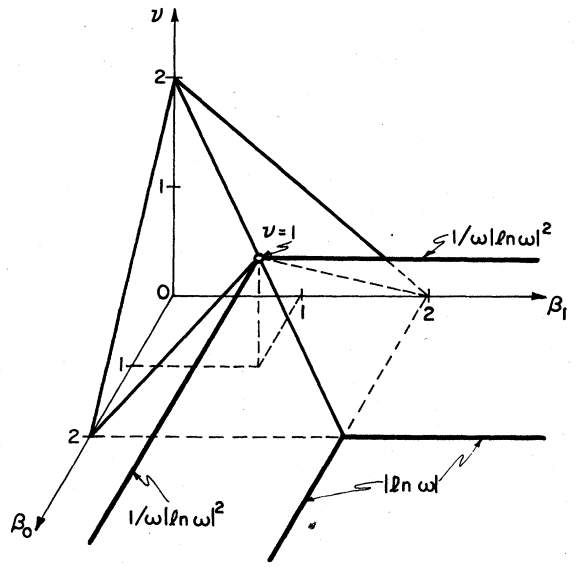

FIG. 5. Variation of ν, where $S(\omega) \sim \omega^{-\nu}$, as a function of β_0 and β_1. The heavy lines indicate singular regions of the function where the frequency dependence of $S(\omega)$ contains logarithmic corrections, as indicated.

D. One-dimensional mappings

We turn now to a discussion of how one can obtain probability distributions corresponding to Eq. (3.4) from a physically realizable mechanism. From the work of Manneville[27] we know that a one-dimensional mapping can generate a signal consisting of a seemingly random alternation between long quiescent intervals and short irregular bursts. We can apply Manneville's ideas to generate a signal consisting of switching events such that the distribution of the time interval between two events obeys a scaling law. Consider the map in Fig. 6 that has two marginally unstable fixed points at $x=0$ and $x=1$, instead of only one marginally unstable fixed point as in Manneville's map. Near each fixed point, the map can be expanded as

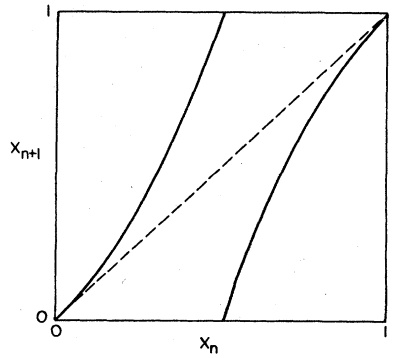

FIG. 6. One-dimensional mapping of the [0,1] interval into itself given by $\Delta X_{n+1} = \Delta X_n(1 + 2\Delta X_n)$, where $\Delta X_n = X_n$ $(0 \le X_n < \frac{1}{2})$, $\Delta X_n = 1 - X_n$ $(\frac{1}{2} < X_n \le 1)$.

TABLE I. Dependence of ν or $S_x(\omega)$ on β_0 and β_1.

β_0, β_1	ν or $S_x(\omega)$
$\min(\beta_0,\beta_1)>2$	$\nu=0$
$\min(\beta_0,\beta_1)=2$, $\max(\beta_0,\beta_1)\geq 2$	$S_x(\omega)\sim \lvert\ln\omega\rvert$
$1<\min(\beta_0,\beta_1)<2$	$\nu=2-\min(\beta_0,\beta_1)$
$\min(\beta_0,\beta_1)=1$, $\max(\beta_0,\beta_1)>1$	$S_x(\omega)\sim 1/\omega\lvert\ln\omega\rvert^2$
$\min(\beta_0,\beta_1)<1$, $\beta_0+\beta_1>2$	$\nu=\min(\beta_0,\beta_1)$
$\beta_0+\beta_1\leq 2$	$\nu=2-\max(\beta_0,\beta_1)$

$$\Delta x_{n+1}=\Delta x_n[1+\lambda(\Delta x_n)^{\alpha}]\ , \tag{3.13}$$

where Δx is the distance to the fixed point. (The figure has been drawn for the particular case $\lambda=2$, $\alpha=1$.) The exponents α and coefficients λ in general differ for the two fixed points, and will be denoted by α_0 and λ_0 for $x=0$ and α_1 and λ_1 for $x=1$. We take as our switching process the signal obtained when we iterate the map $x_n\rightarrow x_{n+1}$, assigning the value 0 or 1 to x when x_n is on the branch corresponding to the fixed point $x=0$ or $x=1$, respectively.

Manneville[27] shows that the probability distribution of the times spent on a branch behaves for long times as

$$\pi(t)=(1+\alpha\lambda t)^{1/\alpha},\quad t\rightarrow\infty \tag{3.14}$$

where the time is in units of the duration of one iteration. We note that a Poisson switching process, that is $\pi(t)=e^{-\lambda}$, corresponds to $\alpha\rightarrow 0$.

Combining Eqs. (3.13) and (3.14) with the results for $\nu(\beta_0,\beta_1)$ shown in Table I, one obtains, in the limit $\omega\rightarrow 0$, the exponent ν of the power spectrum which is a universal quantity depending only on the exponents α_0 and α_1 of the map. The variation of ν with α_0 and α_1 is shown in Table II. In the limit $\alpha_1\rightarrow 0$ where the switching signal degenerates into a random succession of bursts of characteristic duration λ_1^{-1}, we recover the results of Procaccia and Schuster.[28]

We have carried out a numerical test of our predictions for the case $\alpha_0=\alpha_1=1$ which gives an exact $1/\omega$ power spectrum without the logarithmic corrections that one obtains for the Manneville mapping. We iterated the map shown in Fig. 4 on a computer 3×10^6 times for one set of initial conditions and obtained the power spectrum shown in Fig. 7. The sequence of iterates was Fourier transformed over two ranges of frequency to obtain the overlapping sets of spectral estimates shown in the figure. The squares are the averaged results of about 700 individual records of 4096 points each, while the triangles are the averages of about 50 records of 4096 points each, obtained after a tenth-order decimation of the original sequence of iterates. At low frequencies the power spectrum scales as $1/\omega$, down to the lowest-frequency data point.

TABLE II. Dependence of ν or $S_x(\omega)$ on α_0 and α_1.

α_0,α_1	ν or $S_x(\omega)$
$\max(\alpha_0,\alpha_1)<\frac{1}{2}$	$\nu=0$
$\max(\alpha_0,\alpha_1)=\frac{1}{2}$, $\min(\alpha_0,\alpha_1)\leq\frac{1}{2}$	$S_x(\omega)\sim\lvert\ln\omega\rvert$
$1>\max(\alpha_0,\alpha_1)>\frac{1}{2}$	$\nu=2-[\max(\alpha_0,\alpha_1)]^{-1}$
$\max(\alpha_0,\alpha_1)=1$, $\min(\alpha_0,\alpha_1)<1$	$S_x(\omega)\sim 1/\omega\lvert\ln\omega\rvert^2$
$\max(\alpha_0,\alpha_1)>1$, $\alpha_0^{-1}+\alpha_1^{-1}>2$	$\nu=[\max(\alpha_0,\alpha_1)]^{-1}$
$\alpha_0^{-1}+\alpha_1^{-1}\leq 2$	$\nu=2-[\min(\alpha_0,\alpha_1)]^{-1}$

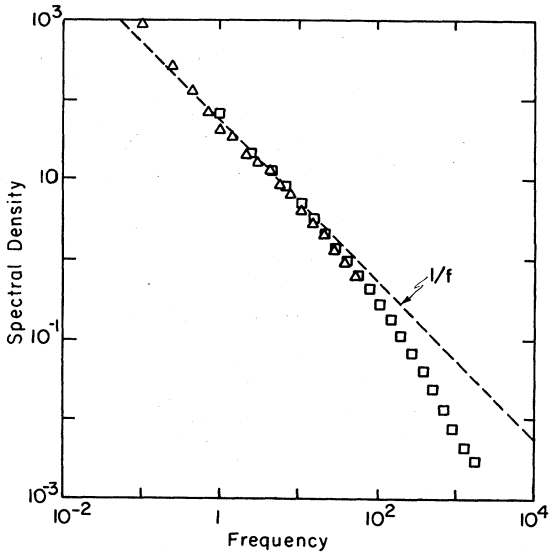

FIG. 7. Power spectrum of the iterates of the mapping of Fig. 6. Different symbols denote different frequency bands for the 4096-point fast Fourier transform.

The mathematical results presented in this section have the following implications for the hopping phenomenon described in Sec. II.

(i) We find that a $1/\omega$ power spectrum can be obtained for widely varying distributions of switching times: It is sufficient that one of the two distributions scales as t^{-1} for long times. The way in which the other decays to zero as $t\rightarrow\infty$ becomes unimportant, although when the exponent β controlling the decay is greater than 1, there is a logarithmic correction to the $1/\omega$ behavior.

(ii) The self-similar property of the spectrum at low frequencies—that is, the absence of any characteristic scale—arises from the mathematical model as a consequence of the precise analytical behavior of the map near the fixed point. One can now understand why the hopping process is so sensitive to changes in the bias current (that change the metastability of the fixed point, that is, the slope of the mapping in the model) and to the addition of noise (that perturbs the equations of motion and destroys the long-term correlations necessary to stay in one mode, smearing out the mapping in the neighborhood of the fixed point).

IV. DIGITAL SIMULATIONS

To investigate whether or not a simple mechanism such as the one presented in Sec. III could arise from the equations of motion of the system and to study the effect of noise and changes in bias current in a quantitative manner, we have performed extensive double-precision di-

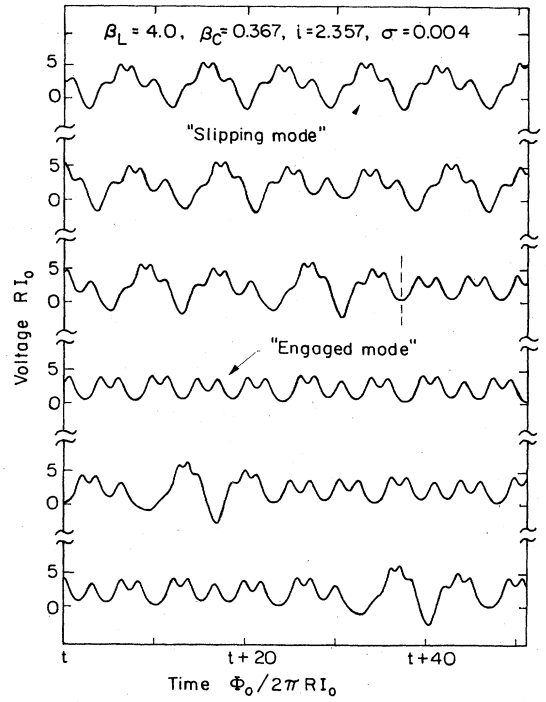

FIG. 8. Representative time sequence (time increasing left to right and top to bottom) obtained by numerical integration of the equations governing the circuit of Fig. 1 for $\beta_L=4.0$, $\beta_C=0.367$, $i=2.357$, $\sigma=0.004$, and $\Gamma=0$. An example of a switching event is indicated by a dashed line separating the two modes, labeled "slipping" and "engaged."

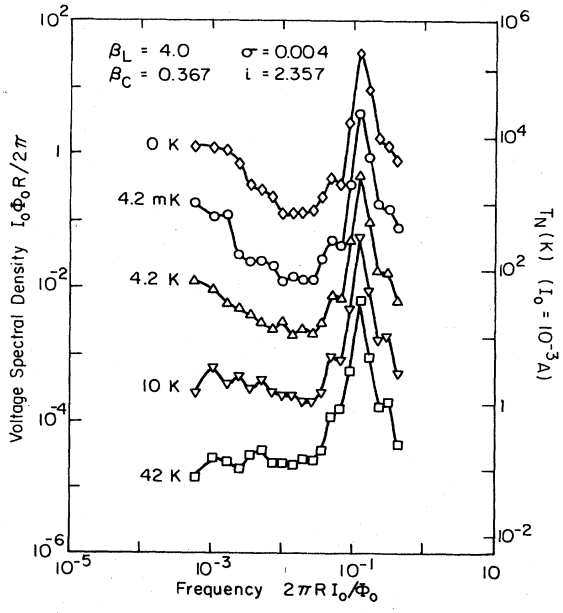

FIG. 9. Power spectra of the voltage for $\beta_L=4.0$, $\beta_C=0.367$, $i=2.357$, and $\sigma=0.004$, for five levels of injected noise. The temperature T associated with each curve is defined by $T=[\Gamma I_0\Phi_0/2\pi k_B]_{I_0=1\text{ mA}}$. The spectral density and noise temperature scales refer to the top curve; scales for the lower curves have been spaced by factors of 10 in power for clarity.

gital computations for a similar set of parameters to those we studied on the analog simulator. We integrated Eqs. (2.6) and (2.7) numerically, using a fourth-order Adams-Bashford-Moulton predictor-corrector method,[29] with typical time steps of 10^{-2} yielding local truncation errors estimated to be $\lesssim 10^{-9}$. For each set of parameters, starting from an arbitrary set of initial conditions, we computed typically 320 Josephson cycles to allow any start-up transients to die out before including the data in power spectra or maps. Figure 8 shows a typical time sequence computed in this way, for parameter values close to those used in Fig. 2, $\beta_L=4.0$, $\beta_C=0.367$, $i=2.357$, $\sigma=0.004$, and $\Gamma=0$. As in the analog simulations, the hopping between the engaged and slipping modes shows up clearly.

The results are presented as voltage spectral densities and Poincaré sections. The voltage spectral densities were computed from the time sequences using a 4096-point fast-Fourier-transform algorithm. Because we are interested only in extremely-low-frequency behavior, the time sequences were first passed through a digital low-pass filter prior to a high-order (typically 100—500) decimation. These filtered time sequences were Fourier transformed and the 2048 harmonics were averaged into 25 frequency bins equally spaced on a logarithmic scale. The results for several such records (typically five) were averaged together. Thermal noise [V_N of Eq. (2.5)] was simulated by the introduction of pseudorandom voltage impulses at each time step; the magnitude of the Fourier transform of these impulses is a constant proportional to $\Gamma^{1/2}$.

Typical power spectra are shown in Fig. 9. The top curve is for $\Gamma=0$, and is the one referenced by the axes. The lower curves are for nonzero Γ, expressed in terms of an equivalent ambient temperature for a junction critical current of 1 mA: $T=(\Gamma I_0\Phi_0/2\pi k_B)_{I_0=1\text{ mA}}$. The lower curves have been successively displaced by 10 dB for clarity. The power spectra at the lowest two temperatures are approximately $1/\omega$ over rather more than one decade, and flat at low frequencies. On the other hand, we see that for $\Gamma=4.2$ K the spectrum has already been modified by the external noise, and that for $T\geq 42$ K, the spectrum is nearly white below 10^{-2}. We can conclude that this level of thermal noise is sufficient to destroy the long-term correlations necessary for $1/\omega$ noise.

The very strong dependence of the low-frequency noise on the value of the bias current (in the absence of added thermal noise) is illustrated in Fig. 10. For $i=2.365$ (solid curve with open circles) the motion consists of a stable subharmonic limit cycle. A slight decrease in the bias current, to 2.361 (solid circles), has little effect on the subharmonic mode, but produces a low-frequency tail that probably indicates the onset of intermittency. When the current is decreased to 2.358 (solid curve), the low-frequency power spectrum is at a maximum, with a $1/\omega$ region. The decrease in bias current from 2.365 to 2.358 (0.3%) has increased the level of noise by over 5 orders of magnitude. A further small decrease in the current

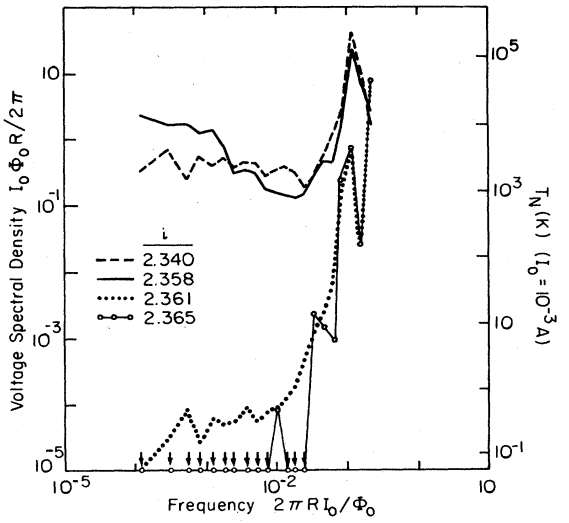

FIG. 10. Power spectra of the voltage for $\beta_L=4.0$, $\beta_C=0.367$, $\sigma=0.004$, $\Gamma=0$, and several values of i. The downward pointing arrows indicate that the noise is less than 10^{-5}.

(dashed curve) produces a low-frequency noise that is white, indicating that the system has become fully chaotic.

To obtain more information on the modes between which the system hops, particularly with regard to the presence of any strange attractors, in Fig. 11 we show a Poincaré section at $\delta=\pi$ for the parameter values used in Figs. 8 and 9. [The choice of this particular section is natural. In either mode, the phase δ passes periodically through the value $\delta=\pi$ with a frequency related to the average voltage via Eq. (2.2), whereas, for example, in the slipping mode, δ passes five times through the value $\delta=0$ during each Josephson period.] The points of the Poincaré section lie on smooth curves indicating that it is one-dimensional as expected for a dissipative system governed

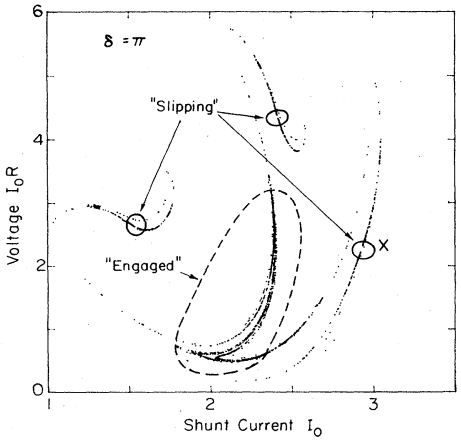

FIG. 11. Poincaré map of the voltage vs shunt current for $\delta=\pi$, $\beta_L=4.0$, $\beta_C=0.367$, $i=2.357$, $\sigma=0.004$, and $\Gamma=0$. The engaged (unstable period one) and slipping (unstable period three) modes are identified.

by a third-order differential equation. When one monitors the time sequences of the iterates, one sees the same behavior as with the analog simulator: The system spends varying amounts of time, that occasionally become very long, in one of two modes. One is the slipping mode, an unstable period-3 limit cycle for which the iterates lie within the encircled regions. Iterates that land near to the fixed points slowly evolve away, as is apparent from the darkened portions of the attractor near the fixed points. The other, engaged mode consists of a chaotic motion along a subsurface of the entire attractor, in the region enclosed approximately by the dashed curve. The points that lie outside these two regions represent transition points between the two modes. (Note that these points, although "transient" in the sense of not belonging to either mode, are still points on the attractor—they do not represent start-up transients.) In that the long-time behavior is determined by the nature of the mapping in the immediate vicinity of the fixed point (the limit cycle of the motion), these transition points can be ignored provided that the mechanism that controls the reinjection into either mode is nearly random.

We have now identified the regions on the Poincaré section corresponding to the two modes. The hopping process is due to the fact that neither region is left invariant by the Poincaré map. Some points in one region have their iterate in the other region. Thus, the distribution of time spent in either mode is a consequence of the properties of the mapping that determine how many iterations the system can make before reaching these transition points. In general, even for a minimal chaotic system such as the one we are studying, the determination of these properties is a difficult problem because the Poincaré map is two-dimensional and may be very intricate. However, we see that in the case of the slipping mode, the Poincaré section is a simple curve which can be parametrized unambiguously by one of the coordinates (we will take the voltage, since this is the variable for which we measured the power spectrum). The Poincaré map then reduces to a one-dimensional mapping, the chaos-producing features of which are explored in the next section.

V. CONSTRUCTION OF THE ONE-DIMENSIONAL MAPPING

We construct the reduced Poincaré map of the points corresponding to the slipping mode in the following way: We take the voltage of a point near the fixed point marked $\times$ in Fig. 11 as the starting voltage V_0 and construct the sequence of voltages of the third iterates of this point: $V_0, V_3, V_6, \ldots, V_n, V_{n+3}, \ldots$ which all lie on a smooth curve. The return map obtained by plotting V_{n+3} versus V_n is illustrated in Fig. 12(a). As the points are generated, they appear alternately on either side of the 45° line. We notice that the map is very nearly one-dimensional, particularly near the fixed point where the mapping intersects the dashed 45° line. The fact that the mapping is very nearly tangential to a $-45°$ line drawn through the fixed point indicates that the loss of stability of this period-3 limit cycle probably occurs via a bifurca-

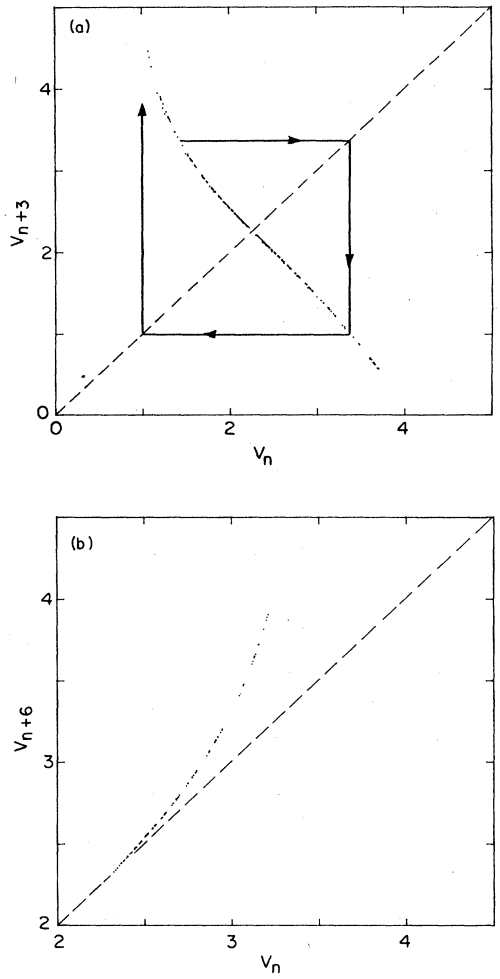

FIG. 12. (a) Return map of the voltage for points near the iterate of the relaxing mode which is identified by a $\times$ in Fig. 11. (b) Second iterate of the mapping in (a), which yields the sixth iterate of the original voltage sequence.

tion with a Floquet multiplier equal to -1. Hence, the mechanism of hopping is similar to a type-III intermittency (Pomeau-Manneville[3]). The departure of the mapping from $-45°$ is approximately linear on the lower branch, and roughly quadratic on the upper branch. The curve shown illustrates how iterates that are injected close to the fixed point inevitably spiral away; this evolution originates in the quadratic shape of the upper branch. We have performed a least-squares fit to the function $V_{n+3}=(-1+\epsilon)V_n+aV_n^2+bV_n^3+cV_n^4$ for the points shown in Fig. 12(a) (the zero of V_n corresponds to the fixed point). We find $\epsilon=-0.025\,28$, $a=0.065\,21$, $b=-0.300\,64$, and $c=0.132\,60$, with a standard deviation of 1.8×10^{-2}.

We now compare the mapping of Fig. 12(a) with the simple model described in Sec. III. We construct a new map, shown in Fig. 12(b), by taking the second iterate of the points on the upper branch of Fig. 12(a): This procedure corresponds to plotting V_{n+6} versus V_n. The similarity between the mapping of Fig. 12(b) and the behavior near the origin in Fig. 6 is striking. The fact that V_{n+6} is very close to a quadratic function provides strong support for the applicability of the model described in Sec. III to the physical system of Fig. 1.

We conclude that, because of the particular functional dependence of the mapping, this system shows a self-similar distribution of times spent in the vicinity of the period-3 limit cycle that explains the $1/\omega$ spectrum. Since only one distribution of hopping times is necessary for a $1/\omega$ spectral density, our ignorance of the mechanism by which the system hops out of the engaged mode does not invalidate our analysis. This unknown mechanism appears to be more complicated because the attractor for the engaged mode consists of many sheets, and it is difficult to see how one could construct a simple mapping that would display the salient features of the metastability of this mode. As a starting hypothesis, Manneville[30] has suggested that a logistic map $x\rightarrow rx(1-x)$ with r slightly greater than 4 might be involved. More work is needed to test this hypothesis.

Finally, there remains the question of what determines the range of the $1/\omega$ region shown in Figs. 2 and 9. We have ruled out significant errors due to the truncations in the numerical methods. One expects a local truncation error Δx_t to give rise to a distortion of the power spectrum at frequencies Δx_t. However, the power spectrum flattens out at frequencies below about 10^{-3}, while Δx_t is about 10^{-9}. The origin of the low-frequency cutoff may be in the requirement that the return map in Fig. 12(a) be analytic in the vicinity of the fixed point. The function V_{n+6} has to be of the form $(-1+\epsilon)^2V_n+a\epsilon(-1+\epsilon)V_n^2+\cdots$, and can never be of the form $V_{n+6}=V_n+AV_n^2+\cdots$ with $A>0$ since the quadratic term obviously vanishes as $\epsilon\rightarrow0$. As a result, this mapping can mimic the ideal mapping of Sec. III only over a limited frequency range. To test whether this explanation of the low-frequency cutoff

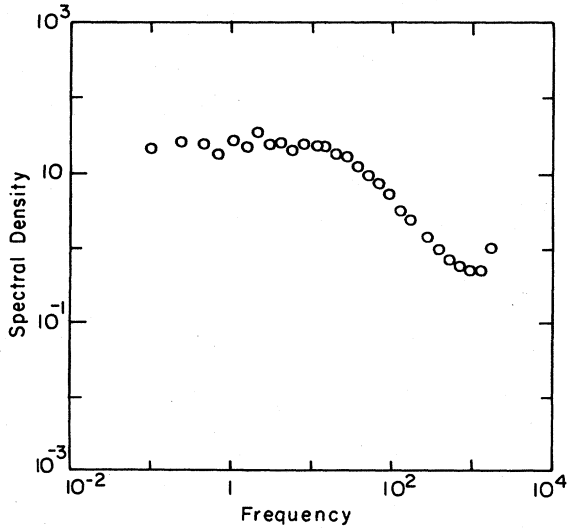

FIG. 13. Power spectrum of the iterates of the mapping $x_{n+1}=(-1+\epsilon)x_n+ax_n^2+bx_n^3+cx_n^4$ where the interval $[-2,2]$ is mapped into itself for $\epsilon=-0.025\,28$, $a=0.065\,21$, $b=-0.300\,64$, and $c=0.132\,60$.

in Figs. 2 and 9 is correct, we have iterated the mapping $x_{n+1}=(-1+\epsilon)x_n + ax_n^2+bx_n^3+cx_n^4$, where x_n is mapped into itself over the range $[-2,2]$, for the values of ϵ, a, b, and c obtained from the least-squares fit to Fig. 12(a). Figure 13 is the power spectrum obtained from 1.4×10^5 iterates of this mapping. We see that the spectrum is flat below a frequency of about 30, unlike the spectrum in Fig. 7 where the $1/\omega$ behavior extended to the lowest frequency, 10^{-1}. We conclude that the low-frequency roll-off in Figs. 2 and 9 very likely arises from similar deviations of the mapping from the ideal case of Sec. III. Consequently, the values of the parameters β_L, β_c, i, and σ could perhaps be adjusted to obtain a successively better approximation to the ideal mapping, resulting in a power spectrum with a $1/\omega$ region extending to lower frequencies.

VI. CONCLUDING SUMMARY

A Josephson tunnel junction, shunted with its self-capacitance and with a resistance in series with an inductance, exhibits the phenomenon of hopping for certain values of the control parameters. Analog simulations show that, although in most cases the hopping is induced by Nyquist noise in the resistor, there is a particular set of control parameters for which, on the contrary, the hopping is suppressed by the thermal noise. This observation suggests that, for this set of parameters, the hopping process between two modes (dubbed "engaged" and "slipping") is deterministic—that is, a consequence of the particular structure of the underlying differential equations—and is not due to the many degrees of freedom of the resistor that acts as a heat reservoir. The power spectrum of the low-frequency noise produced by the hopping is $1/\omega$ over two decades of frequency as demonstrated by analog simulations.

We presented an analytical calculation showing how this particular frequency dependence of the spectrum is related to long-time correlation in the distribution of time intervals between hopping events. These long-time correlations can, in turn, be explained by a phenomenological mathematical model based on the iteration of a simple one-dimensional mapping of the interval [0,1] onto itself.

To investigate how such a simple mapping could arise from the differential equations, we performed a direct numerical integration of these equations. For the same set of control parameters used in the analog simulation, we recovered the hopping behavior characterized by a $1/\omega$ low-frequency spectrum. Using our results for the time sequence of the variables of the junction we can construct a Poincaré map, taking advantage of the fact that the phase difference δ across the junction passes through the value $\delta=\pi$ at regular time intervals. From this Poincaré map, which is two-dimensional, it is possible to extract a one-dimensional mapping that explains the mechanism of hopping from the slipping mode to the engaged mode. This one-dimensional mapping belongs to the class of mapping giving rise to type-III intermittency. Although at the onset of intermittency such mappings generally produce a $\omega^{-1/2}$ power spectrum in the limit $\omega\rightarrow0$, the particular mapping found here has special analytical features near its fixed point that give rise to a ω^{-1} dependence over two decades. It turns out that these features make the mapping closely resemble the ideal phenomenological mathematical model predicting ω^{-1} noise. Furthermore, the small departures of the mapping from the ideal mapping appear to explain the observed low-frequency roll-off of the power spectrum in a satisfactory way. It would be of considerable interest to study deterministic hopping in a real Josephson junction, cooled to a low enough temperature that the effects of Nyquist noise are unimportant.

ACKNOWLEDGMENTS

We wish to thank T. Geisel, M. Goldman, E. Knobloch, R. Littlejohn, P. Manneville, and K. Wiesenfeld for helpful discussions, and E. Knobloch for a critical reading of the manuscript. One of us (M.D.) acknowledges the Commissariat à l'Energie Atomique for partial support during his visit to the University of California, Berkeley. This work was supported by the Director, Office of Energy Research, Office of Basic Energy Sciences, Materials Sciences Division of the U.S. Department of Energy under Contract No. DE-AC03-76SF00098.

*Permanent address: Microelectronics and Computer Technology Corporation, Austin, TX 78759.

†On leave from Service de Physique du Solide et de Résonance Magnétique, CEN Saclay, Orme des Merisiers, 91191 Gif-sur-Yvette Cedex, France.

[1]E. N. Lorenz, J. Atmos. Sci. **20**, 130 (1963); D. Ruelle and F. Takens, Commun. Math. Phys. **20**, 167 (1971).

[2]M. J. Feigenbaum, Physica **7D**, 16 (1983).

[3]Y. Pomeau and P. Manneville, Commun. Math. Phys. **74**, 189 (1980).

[4]G. Iooss, in *North-Holland Mathematical Studies* (North-Holland, Amsterdam, 1979), Vol. 36.

[5]P. Bergé, M. Dubois, P. Manneville, and Y. Pomeau, J. Phys. (Paris) Lett. **41**, L341 (1980).

[6]M. Dubois, M. A. Rubio, and P. Bergé, Phys. Rev. Lett. **51**, 1446 (1983).

[7]H. M. Gibbs, F. A. Hopf, D. L. Kaplan, and R. L. Shoemaker, Phys. Rev. Lett. **46**, 474 (1981).

[8]S. W. Teitsworth, R. M. Westervelt, and E. E. Haller, Phys. Rev. Lett. **51**, 825 (1983).

[9]F. T. Arecchi and F. Lisi, Phys. Rev. Lett. **49**, 94 (1982).

[10]K. Ito, Earth Plan. Sci. Lett. **51**, 451 (1980).

[11]E. Ben-Jacob, I. Goldhirsch, Y. Imry, and S. F. Fishman, Phys. Rev. Lett. **49**, 1599 (1982); I. Goldhirsch, Y. Imry, G. Wasserman, and E. Ben-Jacob, Phys. Rev. B **29**, 1218 (1984).

[12]E. Ott, Rev. Mod. Phys. **53**, 655 (1981).
[13]J. Guckenheimer and P. Holmes, *Nonlinear Oscillations, Dynamical Systems, and Bifurcation of Vector Fields,* in Vol. 42 of *Applied Mathematical Sciences,* edited by F. John, J. E. Marsden, and L. Sirovich (Springer, New York, 1983).
[14]B. D. Josephson, Phys. Lett. **1**, 251 (1962); Adv. Phys. **14**, 419 (1965).
[15]B. A. Huberman, J. P. Crutchfield, and N. H. Packard, Appl. Phys. Lett. **37**, 750 (1980).
[16]R. L. Kautz, J. Appl. Phys. **52**, 3528 (1981); **52**, 6241 (1981).
[17]D. D'Humieres, M. R. Beasley, B. A. Huberman, and A. Libchaber, Phys. Rev. A **26**, 3483 (1982).
[18]T. Geisel and J. Nierwetberg, Phys. Rev. A **29**, 2305 (1984).
[19]E. G. Gwinn and R. M. Westervelt, in *Proceedings of the 17th International Conference on Low Temperature Physics, Karlsruhe, West Germany, 1984,* edited by U. Eckern, A. Schmid, W. Weber, and H. Wuhl (North-Holland, Amsterdam, 1984), p. 1139.
[20]M. Octavio, Phys. Rev. B **29**, 1231 (1984); M. Octavio and C. Readinasser, *ibid.* **30**, 1586 (1984).
[21]R. F. Miracky, J. Clarke, and R. H. Koch, Phys. Rev. Lett. **50**, 856 (1983).
[22]R. H. Koch, R. F. Miracky, and J. Clarke (unpublished).
[23]K. Wiesenfeld, E. Knobloch, R. F. Miracky, and J. Clarke, Phys. Rev. A **29**, 2102 (1984).
[24]The circuit simulating the Josephson junction was the model JA-100, manufactured by Philipp Gillette and Associates, Beaverton, Oregon. To this, a combination of active and passive elements was added to represent the complete circuit of Fig. 1.
[25]D. G. Dempsey, M. T. Levinsen, and B. T. Ulrich, IEEE Trans. Magn. **MAG-11**, 811 (1975).
[26]*Handbook of Mathematical Functions,* Natl. Bur. Stand. (U.S.) Appl. Math. Ser. No. 55, edited by M. Abramowitz and I. A. Stegun (U.S. GPO, Washington, D.C., 1964).
[27]P. Manneville, J. Phys. (Paris) **41**, 1235 (1980).
[28]I. Procaccia and H. Schuster, Phys. Rev. A **28**, 1210 (1983).
[29]J. D. Lambert, *Computational Methods in Ordinary Differential Equations* (Wiley, New York, 1973).
[30]P. Manneville (private communcation).